InGaAs/AlGaAs ridge waveguide lasers utilizing an InGaP etch-stop layer



1992 Semicond. Sci. Technol. 7 1425

(http://iopscience.iop.org/0268-1242/7/11/024)

Semicond. Sci. Technol. 7 (1992) 1425–1427. Printed in the UK

LETTER TO THE EDITOR

# InGaAs/AlGaAs ridge waveguide lasers utilizing an InGaP etch-stop layer

**W S Hobson, Y K Chen and M C Wu**

AT&T Bell Laboratories, Murray Hill, NJ 07974, USA

Received 24 August 1992, accepted for publication 1 September 1992

**Abstract.** An InGaP etch-stop layer was used to control the mesa height in a ridge waveguide InGaAs/AlGaAs strained multiple quantum well laser grown by organometallic vapour phase epitaxy. These 950 nm lasers exhibited internal quantum efficiencies of $\eta_i = 0.99$ and very low internal losses of $\alpha_i = 2.6\ \mathrm{cm}^{-1}$. For a cavity length of 500 $\mu$m, a threshold current of 12 mA was obtained. The high performance of these lasers and the improved uniformity of their characteristics demonstrate the utility of InGaP etch-stop layers in improving process yield without detrimental effects.

There is considerable interest in InGaAs/AlGaAs strained quantum well lasers for applications within the 0.9–1.1 $\mu$m wavelength range, such as high power pump lasers for Er-doped fibre amplifiers and rare-earth-ion solid state lasers, obtaining blue-green laser emission by frequency doubling, and optoelectronic integrated circuits [1–10]. Ridge waveguide (RWG) lasers are in principle the simplest way to achieve high power fundamental mode performance. However, it is imperative to control the ridge height since this determines the index-guiding of the laser. If the ridge is underetched, the laser will not be index-guided and the threshold current will increase significantly [11]. Overetching of the ridge will result in the laser exhibiting multiple lateral modes. The usual procedure is to use timed etching to control the ridge height. However, invariably the etching across the wafer is non-uniform, thereby leading to poor yield. A recent report has successfully demonstrated the use of an AlAs etch-stop layer which allowed selective etching of the $Al_{0.22}Ga_{0.78}As$ cladding layer [12]. We have used $In_{0.49}Ga_{0.51}P$ (hereafter referred to as InGaP) as an alternative etch-stop layer. This approach takes advantage of the excellent selectivity between InGaP and AlGaAs and permits the use of any AlGaAs composition in the cladding layer.

The InGaAs/AlGaAs laser structure was grown in an atmospheric pressure vertical-geometry reactor described previously [13]. Hydrogen was used as the carrier gas. Arsine and phosphine were used as the As and P precursors, while trimethylgallium, trimethylaluminium and trimethylindium were utilized as the gallium, aluminium and indium sources respectively. Disilane and diethylzinc were the Si and Zn dopant precursors respectively. A constant GaAs growth rate of 25 nm $\mathrm{min}^{-1}$ was used throughout the growth. The epitaxial layer structure is given in table 1. The $n^+$-GaAs buffer, n- and p-$Al_{0.4}Ga_{0.6}As$ cladding layers and undoped $Al_xGa_{1-x}As$ ($x = 0.4$–$0.1$) graded index separate confinement layers were grown at 700 °C, and the InGaAs/GaAs multiple quantum well active layer, InGaP etch-stop layer and $p^+$-GaAs contact layer were grown at 625 °C. Growth interruptions were used in order to allow time for the temperature changes. The 3 nm thick p-GaAs layer grown prior to the InGaP layer was used to prevent oxidation of the p-$Al_{0.4}Ga_{0.6}As$ surface upon cooling to 625 °C.

**Table 1.** Epitaxial layer structure of the InGaP etch-stop InGaAs/AlGaAs multiple quantum well laser.

| Layer composition | Thickness (nm) | Doping concentration ($p, n$: $10^{18}\ \mathrm{cm}^{-3}$) |
|---|---|---|
| GaAs | 200 | $p = 10$ |
| $Al_{0.4}Ga_{0.6}As$ | 1350 | $p = 1.0$ |
| InGaP | 7 | $p = 1.0$ |
| GaAs | 3 | $p = 1.0$ |
| $Al_{0.4}Ga_{0.6}As$ | 150 | $p = 1.0$ |
| $Al_xGa_{1-x}As$ ($x = 0.1$–$0.4$) | 180 | undoped |
| $In_{0.20}Ga_{0.80}As$/GaAs MQW active layer | 8/20 | undoped |
| $Al_xGa_{1-x}As$ ($x = 0.4$–$0.1$) | 180 | undoped |
| $Al_{0.4}Ga_{0.6}As$ | 1500 | $n = 1.0$ |
| GaAs | 500 | $n = 2.0$ |

A schematic diagram of the self-aligned RWG InGaAs/AlGaAs MQW laser is shown in figure 1. The InGaP etch-stop layer was located 0.15 $\mu$m above the active layer. The 3 $\mu$m wide ridge was formed by wet

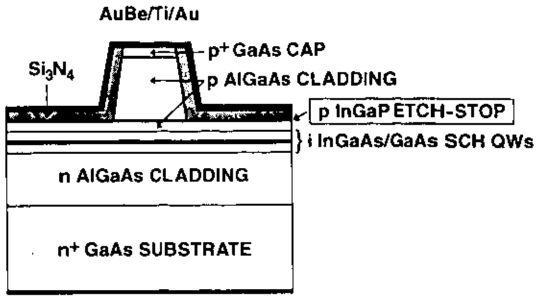


**Figure 1.** Schematic diagram of the self-aligned ridge waveguide GRINSCH laser with an InGaP etch-stop layer in the p-AlGaAs cladding layer.

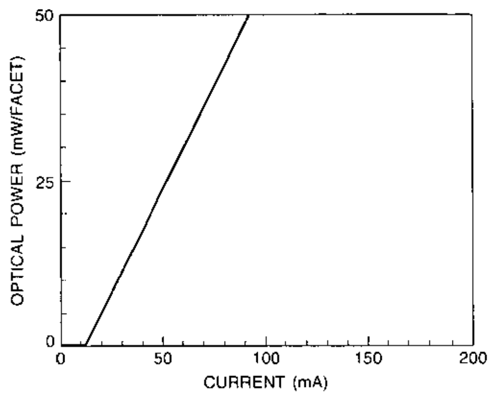


**Figure 2.** The room-temperature cw *L–I* characteristic for the 3 $\mu$m × 500 $\mu$m RWG GRINSCH laser with InGaP etch-stop layer.

chemical etching using 1:1:10 $H_2SO_4$:$H_2O_2$:$H_2O$ cooled to 4 °C, which produced an etch rate of 200 nm min$^{-1}$ and resulted in a very smooth surface. After the etching step, a CVD $Si_3N_4$ layer was deposited to passivate the etched surface. The wafer was thinned down to 100 $\mu$m and AuBe/Ti/Au or Au/Sn/Au metal layers were evaporated for p and n contacts respectively. The individual lasers were obtained by cleaving the wafer into stripes of various lengths and were mounted junction side up on copper heat sinks.

A typical continuous-wave light–current ($L$–$I$) characteristic of a 500 $\mu$m long cleaved-facet InGaP etch-stop RWG InGaAs/AlGaAs is shown in figure 2. The threshold current was 12 mA and the differential quantum efficiency was 42.7% per facet. The lasing wavelength was centred at 950 nm for $I = 1.6I_{th}$. Output power was limited by the catastrophic optical damage threshold of ~ 30–40 mW per $\mu$m of stripe width. Several lasers across the 2 inch (51 mm) diameter were tested and were found to have nearly identical $L$–$I$ characteristics. This was in marked contrast to our usual timed-etch processing.

The cavity length dependence of the quantum efficiency $\eta$ is given by

$$\eta^{-1} = \eta_i^{-1}[1 + \alpha_i L_c / \ln(1/R)] \qquad (1)$$

where $\eta_i$ is the internal quantum efficiency, $\alpha_i$ is the internal loss and $R = \sqrt{R_1 R_2}$ where $R_1$ and $R_2$ are the two facet reflectivities [13]. The value of $\eta_i = 0.99$ is obtained by extrapolating the inverse external differential

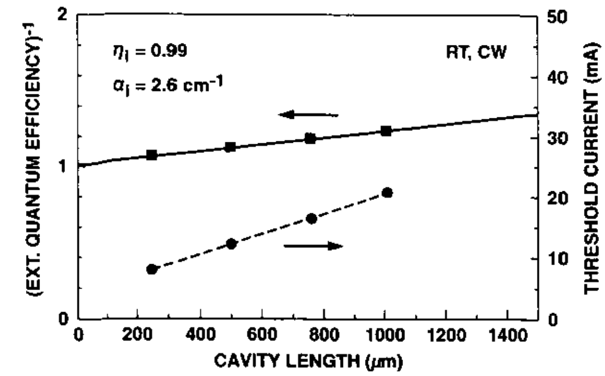


**Figure 3.** The inverse differential quantum efficiency and threshold current as a function of cavity length for the InGaP etch-stop/GRINSCH lasers.

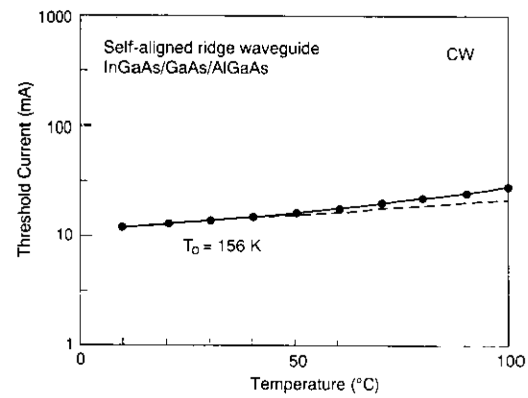


**Figure 4.** The threshold current as a function of temperature for a 3 $\mu$m × 500 $\mu$m RWG GRINSCH laser with InGaP etch-stop layer.

quantum efficiency to zero cavity length. An extremely low internal loss of $\alpha_i = 2.6$ cm$^{-1}$ was determined from the slope of the linear fit. The values of $\eta_i$ and $\alpha_i$ obtained here are comparable to the best achieved for InGaAs/AlGaAs lasers [2, 7, 10], indicating that the InGaP etch-stop layer does not have a detrimental effect on the loss mechanisms. Also shown in figure 3 is the threshold current as a function of cavity length. For a cavity length of $L_c = 500$ $\mu$m the threshold current was 12 mA, while for $L_c = 1000$ $\mu$m the threshold current was 20 mA. The threshold current as a function of temperature for the 3 $\mu$m × 500 $\mu$m RWG InGaAs/AlGaAs laser (with InGaP etch-stop layer) operated CW is given in figure 4. A characteristic temperature of $T_0 = 156$ K was measured over the temperature range 10–50 °C. This reflects, in part, the excellent carrier confinement of this laser structure.

In summary we have demonstrated the use of an InGaP etch-stop layer to provide a convenient means for controlling the etching process in fabricating RWG structures. High performance lasers were obtained, indicating that there were no detrimental effects from the presence of the InGaP layer. This approach should also apply to dry chemical processing such as reactive ion etching where excellent selectivity between InGaP and (Al)GaAs is easily achieved.

The authors acknowledge the technical assistance of L J Oster and the continued support of S S Pei, W T Tsang and D V Lang.

## References

[1] Camras M D, Brown J M, Holonyak N, Nixon M A, Kaliski R W, Ludowise M J, Dietze W T and Lewis C R 1983 *J. Appl. Phys.* **54** 6183
[2] Choi H K and Wang C A 1990 *Appl. Phys. Lett.* **57** 321
[3] Evans G A *et al* 1989 *Appl. Phys. Lett.* **55** 2721
[4] Fekete D, Chan K T, Ballantyne J M and Eastman L F 1986 *Appl. Phys. Lett.* **49** 1659
[5] Laidig W D, Caldwell P J, Lin Y F and Peng C K 1984 *Appl. Phys. Lett.* **44** 653
[6] Laming R I, Farries M C, Morkel P R, Reekie L, Payne D N, Scrivener P L, Fontana F and Righetti A 1989 *Electron. Lett.* **25** 12
[7] Larsson A, Cody J and Lang R L 1989 *Appl. Phys. Lett.* **55** 2268
[8] Mears R J, Reekie L, Poole S B and Payne D N 1987 *Electron. Lett.* **23** 1026
[9] Uehara S, Okayasu M, Takeshita T, Kogure O, Yamada M, Shimizu M and Horiguchi M 1990 *Optoelectronics* **5** 71
[10] Williams R L, Dion M, Chatenoud F and Dzurko K 1991 *Appl. Phys. Lett.* **58** 1816
[11] Shieh C, Mantz J, Lee H, Ackley D and Engelmann R 1989 *Appl. Phys. Lett.* **54** 2521
[12] Elman B, Sharfin W F, Crawford F D, Rideout W C, Lacourse J and Lauer R B 1991 *Electron. Lett.* **27** 2032
[13] Thompson G H B 1980 *Physics of Semiconductor Laser Devices* (Chichester: Wiley) pp 96–8